ORIGINAL PAPER

Salinization of groundwater during 20 years of agricultural irrigation, Luxor, Egypt

Ibrahim Said [iD] · **Salman A. Salman** · **Ahmed A. Elnazer**

Abstract Groundwater salinization is a global problem accounting for 11–30% of the world's irrigated areas. Luxor region in Upper Egypt is one of such areas affected by salinity. Multivariate statistics indicate that groundwater is affected by intermixed processes; mineralization (salinization), fertilization, domestic wastes, and meteoric recharge. Temporal change in salinity and hydrochemical facies during 1997–2017 revealed aquifer salinization, due to the dissolution of salts from overlain saline soil and marine deposits underneath as well as up-coning of deep saline water. Increasing salinity over time was statistically documented, exhibited temporally high significant differences ($P < 0.05$), where salinization consumed a quarter of the aquifer during 20 years. Evolution of water facies from less mineralized Ca–Cl, Mg–Cl to highly mineralized Na–Cl species explains the salinization process over time. Elevated content of Na and Cl is associated with the dissolution of marine sediments and saltwater intrusion. The shift from silicate weathering into evaporation dominance confirmed the saltwater intrusion. As a result, groundwater has a high degree of salinity, is not suitable for domestic and other uses. On other hand, fertilization and domestic sewage are probably responsible for the high NO_3^- and Cd content. Over 80% of Cd exists in mobile species facilitates Cd-plant uptake indicating an alarming environmental situation. Cd mobility is closely related to elevated salinity and chlorinity, allowing competition with major ions and forming of soluble complexes. The present approach will improve the uncertainties of environmental interpretation, as an initial step for aquifers management in reclaimed lands.
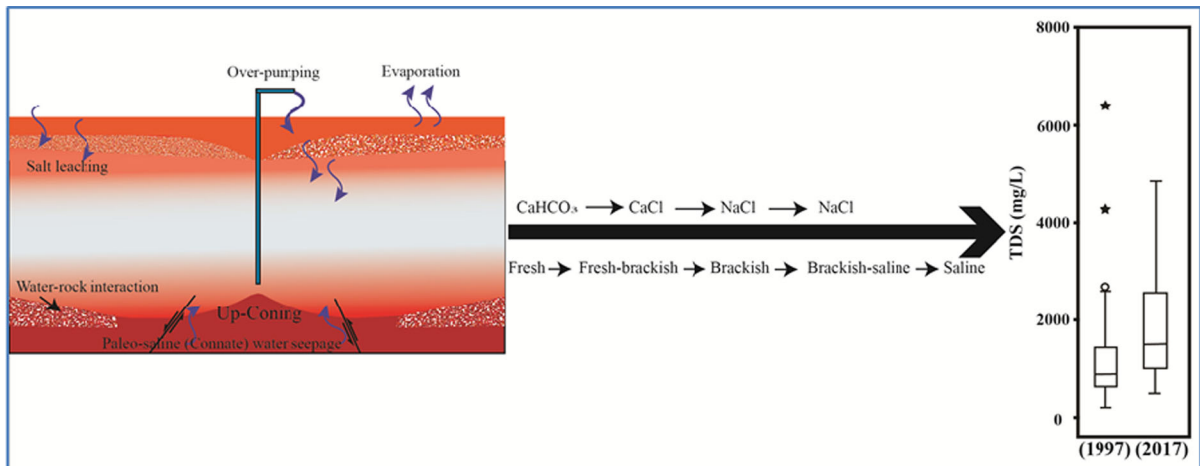
I. Said (✉) · S. A. Salman · A. A. Elnazer
Department of Geological Sciences, National Research Centre, Dokki, Cairo, Egypt
e-mail: hemanrc@gmail.com

I. Said · S. A. Salman · A. A. Elnazer
Geological Sciences Department, National Research Centre, 33 El Bohouth St. (Former El Tahrir St.), POB 12622, Dokki, Giza, Egypt

Graphical abstract

Introduction

This paper was designed to compare the change in groundwater quality during 1997–2017 in one of the Egyptian regions; Luxor area. In arid regions, groundwater is wealth that should be protected. Water scarcity is not only limited to quantity, but also to quality, as unfit for use is lost water. Geochemical processes occurring in the aquifer play a basic role in the spatio-temporal variation of water quality. Hence, identifying the processes controlling groundwater quality is an essential step toward aquifer management. One of the most important factors that deteriorate groundwater quality is salinization. Groundwater salinization is a global problem and a major environmental issue (Greene et al., 2016). Salinity is currently growing at a rate of 10% per year (Krishan, 2019). Numerous studies documented groundwater salinization worldwide, in South America (Bocanegra et al., 2010); Australia (Werner, 2010); In Africa: Morocco (El Halimi et al., 2001), Libya (Alfarrah & Walraevens, 2018), Egypt (Sherif, 1999, Abd-Elhamid et al., 2016, Sharaky et al., 2017, Said et al., 2020 and

Said & Salman, 2021); In Europe (Essink, 2001 and VAndenBOHede et al., 2015).

Irrigation is one of the main factors affecting groundwater salinity in arid and semi-arid regions (Williams, 2001). Intensive irrigation significantly modifies the hydrological cycle, where it is a major source of groundwater recharge, and it mobilizes the geogenic salinity from the deeper connate under excessive pumping (Foster et al., 2018). 11–30% of the global irrigated areas are affected by salinity (Pulido-Bosch et al., 2018). Globally, 38–43% of agricultural land depends on groundwater (Siebert et al., 2010 and FAOSTAT, 2016). Since the 1950s, the amount of irrigation water withdrawn has doubled and is expected to increase by 14% by 2030 (FAOSTAT, 2016 and Pulido-Bosch et al., 2018). About 30% of global irrigation water withdrawals flow back to groundwater and rivers (Scanlon et al., 2007). This affects negatively the groundwater quality where it leads to the leaching of agrochemical pollutants and surface soil salts inside the aquifers. On other hand, the up-coning phenomenon is a well-known salinization mechanism that occurs as a result of over pumping, where saline water rises to replace the freshwater withdrawn. In such case, the saline water rises by 40 units for every unit of the freshwater withdrawn (Velmurugan et al., 2020). The excessive extraction of groundwater has led to the depletion and degradation of aquifers in Egypt. Excessive pumping in the Nile Delta aquifer activates saline water up-coning causing

groundwater salinization (Sharaky et al., 2017). Seawater intrusion has been detected 60 km inland as a result of over pumping in Nile Delta (Sherif, 1999). Thus, salinization resulting from agricultural activities is an urgent problem with the greatest environmental and economic impacts (Morris et al., 2003 and FAO, 2011).

Egypt has expanded desert agriculture to meet food needs as the population increases. This causes pressure on the groundwater; the main source of irrigation water in the desert lands. Although the Nile River share of 55.5 billion m^3/year (CAPMAS, 2020), Egypt faces water scarcity with increasing demand. Freshwater share per capita decreased from 2,189 m^3/capita/year in 1966 to 1035 m^3/per capita/year in 1990 and is expected to decline to 536 m^3/capita/year by 2025 (El-Gohary, 2011). Mazzoni et al., 2018 predicted that Egypt will face severe water depletion by $\sim 45\%$ in 2050. Approximately 12% of the total water resources in Egypt come from groundwater; 6.1 BCM/yr from the Nile aquifer (Abd Ellah, 2020) plus 1.65 BCM/yr from other non-renewable groundwater (Abdel-Shafy & Kamel, 2016). Agricultural irrigation consumed 41% of the total groundwater abstracted in Egypt (Margat & der Gun, 2013). The excessive groundwater extraction caused the depletion of water, as the groundwater in Egypt is not renewable because of aridity. The percent of withdrawals to total renewable groundwater resources in Egypt equals 350% (Giordano, 2009), which is a large percentage compared to the United State (8.5), India (45.3), China (6.4), Germany (15.2), France (6.0), Spain (16.7), and Japan (51.9). This hydraulic gradient activates the upconing and salinization processes. Thus, agricultural irrigation contributes to the depletion and deterioration of groundwater quality. It is necessary to assess the phenomenon of groundwater salinization to open up various options for rational utilization of groundwater resources in this semi-arid region to avoid deterioration of the groundwater quality.

The current study discusses the hydrochemical processes affecting groundwater quality with special reference to the bioavailability of potentially toxic elements (Cd and Pb). Samples were collected and analyzed for ions. The data were analyzed using statistical models and a few well-known water quality/chemistry models. Multivariate statistic helps to explain the key processes affecting groundwater quality by reducing and categorizing data. Although multivariate statistic does not establish direct cause-effect relationships (Yidana et al., 2012), it provides helpful links facilitates unveiling the hidden relationships between geo- and environmental data (Said et al., 2020). PCA reduces large data sets in a fewer number of factors to facilitate their interpretation. Of course, data reduction comes at the expense of accuracy, but it is the trick to catch the basic processes controlling water chemistry. PCA reduces the dimensions of data sets, increases interpretability but at the same time reduces information loss (Jolliffe & Cadima, 2016). So the idea of PCA is simply to reduce large data to a fewer number of variables while preserving as much information as possible. Geochemical reactions during salt/freshwater mixing are usually followed by a change in ions concentration and/or hydrochemical facies. Piper (1944) diagram helps to detect salinization/ freshening processes by tracking change in ion ratios and hydrochemical facies. Meteoric waters predominate the bicarbonate types, while saltwater predominates the chloride water type with mixed cation composition. Such hydrochemical facies depend on the nature of rock encountered, and help to examine the evolution of a groundwater system. On other hand, groundwater quality is held by dissolution/precipitation processes and the chemical form of the potentially toxic elements (PTEs) controlling their bioavailability. In this regard, mineral saturation and metals speciation were calculated as part of modeling software output named Visual MINTEQ 3.1 (Gustafsson, 2011). This model is useful for predicting metal bioavailability and the dissolution/precipitation of minerals into or from the aquifer system based on saturation index (SI) value; the matter affects groundwater composition. The mineral is in the precipitation, equilibrium, and dissolution state with SI > 0, = 0, and < 0, respectively (Said et al., 2020). Metal speciation plays a key role in bioavailability and toxicity. The toxic effect of metals in solution is a function of their species rather than their total concentrations, because the plant uptake of elements is restricted to the dissolved phases. Therefore, PTEs bioavailability and biological uptake can be better understood in terms of their chemical speciation. Based on metals to ligands concentrations, V. MINTEQ 3.1 can predict the distribution of PTEs species, in free ion, inorganic complexes, and precipitated phases.

Materials and methods

Study area

Luxor in Upper Egypt was a city belonging to the Qena governorate, and it was administratively separated in 2009 to become a new governorate called Luxor Governorate. The study area (1300 Km^2) is located in the high arid desert of Luxor in Egypt, between latitude 25° 14′ 00″ and 26° 1′ 17″ N and longitude 32° 22′ 30″ and 32° 45′ 00″ E (Fig. 1). The desert fringes are partially reclaimed and are used mainly by agriculture that depends on groundwater. Given the impact of the region's geology and hydrogeology on groundwater composition, they have been summarized here using previous studies (Said, 1962, EGSM, 1981, Said, 1990, Omer, 1996, RIGW, 1997, Omran et al., 2001, Ismail et al., 2005, Elwaseif et al., 2012, Said, 2012, and El Alfy et al., 2019).
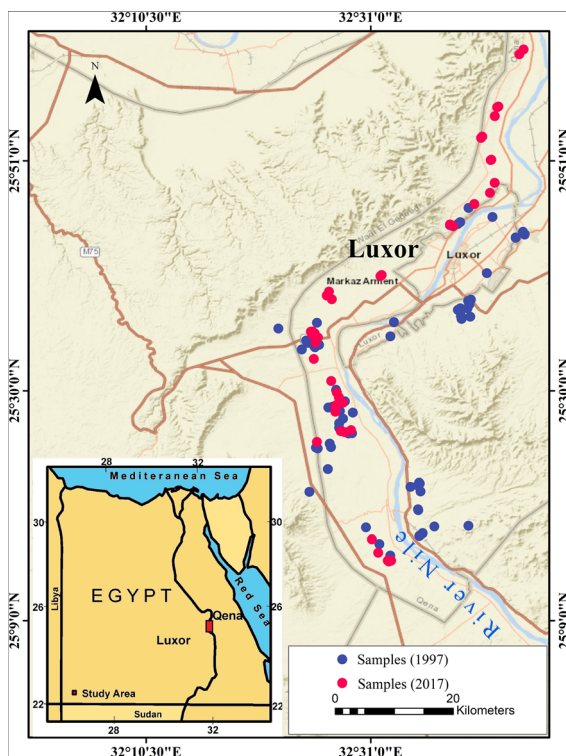
Geology

The stratigraphic sequence of the aquifer system varies from the lower cretaceous to recent (Fig. 2). From Cretaceous to middle Eocene age, Egypt was covered by the Mediterranean Sea till Esna area in Aswan, as a result of a downward movement. During that period, the sea gradually deepened, leaving sediments of different depositional environments. In the beginning, the sea was shallow, so the sandy coastal sediments were formed, known as the Nubian Sandstone, and with the continuous dropping in the land level, the sea grew deeper, forming deeper deposits on its bottom; the mudrocks and then the chalky rocks. This gradual deepening of the sea that accompanied the downward movement is most clearly seen in the presence of shallow deposits of lower Cretaceous (Nubian sandstone) covered with deeper deposits (Shale and marl) of the Upper Cretaceous period (Fig. 2). Followed by Paleocene shale and Eocene limestone plateau. Before the end of Eocene age, the Egyptian lands had uplifted; the Tethys withdrew northerly giving the late-middle Eocene regressive facies. In Pliocene age, Atlantic Ocean connected with the Mediterranean, so an arm extended from the sea to the Nile Valley (from Cairo to Aswan), and the Nile Valley was like a bay of the Mediterranean Sea, this resulted in the formation of Pliocene marine deposits. In Plio-Pleistocene period, arid conditions prevailed, except from some seasonal rains, forming lacustrine deposits (carbonate and clastic facies), named Issawia formation. While Pleistocene was the Ice Age in Europe, it was marked in Egypt by the abundance of rain. These Pleistocene rains carried sediments from Eastern Desert Mountains (local deposits) and Ethiopian plateau forming Pleistocene water-bearing formations, mainly of sand

Fig. 1 Groundwater sample map of Luxor area
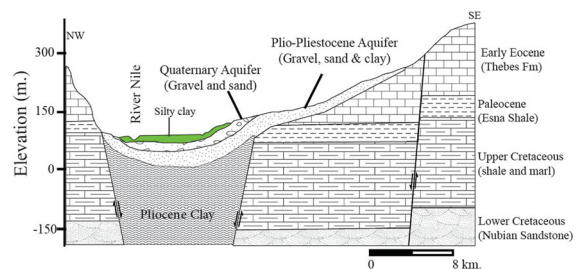
Fig. 2 Hydro-geologic cross-section at Luxor area (After RIGW, 1997)

and gravel deposits. In late-middle Pleistocene period, dry climatic conditions prevailed and the Nile water was restricted to that coming from Ethiopia in the form of a river suspended load (silt and clay) forming the flood plains in the Nile Valley, these deposits are referred to as Dandara formation. Finally, Holocene deposits, which are still forming today, represented by silt and clay in the Nile Valley region (the modern River Nile sediments and Akrin formation), disappear into the desert lands, turning into wadis sediments (reworked pre-existing clastic and carbonate deposits). The absence of the silt–clay layer toward the desert fringes is what makes the unconfined desert aquifer unlike the semi-confined one at the floodplain area.

Hydrogeology

Quaternary aquifer is a part of graben system in which the water-bearing sediments fault against the older sediments of Cretaceous, Tertiary, and connected with the deeper aquifers via fault planes (Fig. 2). Quaternary aquifer consists of Pleistocene water-bearing layer (gravel and sand intercalated with lenses of clay) sandwiched between Pliocene marine sediments and Holocene silty-clay layer. Quaternary aquifer has a local thickness ranging from 5 to 95 m. Aquifer is unconfined in desert areas due to the absence of silty-clay layers of Holocene. The main recharging sources are Nile River (at floodplain area), irrigation return, deep aquifers, and leakage from septic tank. Rainfall is not a significant contribution in recharging process due to the arid climate. Annual rainfall < 5 mm/y against higher evapotranspiration rate (185 cm/y). The main discharge source is pumping wells.

Sampling and analyses

Two data sets of groundwater samples were taken from pumping wells in Luxor area, Egypt (Fig. 1). A total of 66 groundwater samples dating back to 1997 (from well owners) and 43 groundwater samples were collected in 2017. The samples were collected following the groundwater sampling protocol set out by Weaver (1992). Each well was pumped for 20 min before sampling; a1 liter plastic bottle was rinsed three times with water to be sampled and packed to the brim, to include as little air as possible at the top of the bottle, then closed tightly. The samples were saved in

icebox at a temperature of < 4 °C. The samples were then placed in fridges and transported back to the laboratories of NRC for analysis.

The temperature, pH, TDS and, electrical conductivity (EC) were determined in situ using a digitally combined electrode (HANNA HI 991,300, UK) which was calibrated prior to taking the readings. In the laboratory, the samples were filtered using Whatman ashless filter paper No. 42, England, and analyzed for chemical constituents according to standard procedures of APHA (1995). Full water analysis was performed one day after sampling, stored at 4 °C. Sodium and potassium were determined by spectrophotometer Total hardness (TH) as $CaCO_3$, carbonate, bicarbonate, and chloride were analyzed by volumetric methods. Sulfate and nitrate were determined by using Spectrophotometer (HANNA HI 83,215, UK). Cd and Pb were analyzed by using the Inductively Coupled Plasma- Mass Spectrometry (ICP-MS) (iCAP-Q, Thermo Scientific Series, USA) after acidifying samples with HNO_3 to pH < 2. Blanks and standard solution (Merck ICP multi-element standard solution IV) were used for analyses validation and quality assurance with three replicates of each sample. The recovery of samples with respect to reference material was 90–105%, indicating the effectiveness and high accuracy of the analyses process.

Charge balances were employed to verify the accuracy of chemical analyzes. The error was less than 5% for all samples analyzed indicating good analysis accuracy overall.

Statistical analysis and hydrochemical models

All statistical analysis of the groundwater components was conducted using SPSS 16.0 software. Descriptive statistics were performed to understand the distribution of data, followed by Principle component analysis (PCA) to outline the main factors affecting groundwater quality. Measuring Kaiser–Meyer–Olkin for the adequacy of the sampling (KMO MSA) = 0.659 higher than the minimum requirements of 0.5, with Bartlett's sphericity test (0.00), is less than the significance level recommended by Kaiser, 1960 and Tabachnick & Fidell, 2007. This means that the data is suitable for Principle component analysis.

Visual MINTEQ 3.1 is a thermodynamic program is used to predict metal speciation and state of mineral

phases, hence, enrichment/ depletion process and pollutant bioavailability. Inputs of the software are pH and water composition (ion concentrations). Piper (1944) diagram is a powerful tool for identifying various hydrochemical facies, helping to track intrusion/refreshing processes. Piper (1944) diagram was created based on the predominant anions and cations, using RockWare Aq.QA software (V. 1.1, 2005).

For rock-water interaction, Gibbs and End-member charts have been used. Salinization process was evaluated by Revelle, 1941 (Eq. 1). According to Karunanidhi et al., 2020, groundwater with RI values > 0.5 is said to be influenced by salinization. Chloro-alkaline indices CAI1 (Eq. 2) and CAI2 (Eq. 3) (Schoeller, 1965) were applied to deduce ion-exchange activity in groundwater. Positive CAI1 and CAI2 is indicative of reverse ion-exchange reaction where Na and K replace Ca and Mg ions leading to the increase of Ca and Mg concentration in groundwater, whereas it becomes forward ion-exchange reaction when CAI1 and CAI2 values are negative with Ca and Mg replacing Na and K leading to the increase of Na and K concentration in groundwater. Moreover, if CAI1 and/or CAI2 are zero, it indicates ion exchange does not occur during the formation of the groundwater. Besides, the larger the absolute values of CAI1 and CAI2 are, the stronger the ion-exchange interaction is (Kaur et al., 2019).

$$RI = Cl/(HCO_3 + CO_3) \tag{1}$$

$$CAI\,1 = (Cl - (Na + K))/Cl \tag{2}$$

$$CAI\,2 = (Cl - (Na + K))/(SO_4 + HCO_3 + CO_3 + NO_3) \tag{3}$$

Result and discussion

Descriptive statistic

Analytical data are shown in Table 1 and Fig. 3 for two periods; 1997 and 2017. Great temporal variation in water chemistry was noticed between the studied two periods. The cations have the same decreasing order, Na > Ca > Mg > K, in the two periods, while anions were Cl > HCO_3 > SO_4 during 1997 and

$SO_4 > Cl > HCO_3$ during 2017. Water salinity average varies from 1280.6 ± 997.2 mg/L in 1997 to 1828.6 ± 1124.7 mg/L in 2017, which is above WHO, 2017 recommended limit (1000 mg/L). Despite the relatively high salinity in most of the samples, 50% (1997) and 25% (2017) of the samples are drinkable. 75% (1997) and 50% (2017) of the sampled wells are suitable for irrigation compared to FAO, 1994 (2000 mg/L). TDS exhibited a medium variation coefficient (CV = 77.9% and 61.5%) attributed to the difference in the land use, hydrological and lithological characteristics along the aquifer area. Water temperature was changed from 25.8 °C in 1997 to 29.4 °C in 2017. The temperature of water is related to climatic temperature and has great influence on water chemistry and biology. The increase in water temperature can be attributed to the increase in ambient air temperature; which increases about 0.82 °C in the last 20 years (Mostafa et al., 2019). The recorded decrease in pH by a value of 0.5 pH (from 1997 to 2017) is an indicator of the groundwater acidification. The groundwater acidification may be attributed to the weak buffering capacity of the aquifer. Buffering capacity is dependent on water alkalinity (CO_3 and HCO_3 levels), it was noticed that water levels of anions were changed from $Cl > HCO_3 > SO_4$ during 1997 to $SO_4 > Cl > HCO_3$ in 2017 with the increase in strong acid radicals SO_4 and Cl than HCO_3 indicating the exhaust of buffering capacity. The increase in SO_4 and Cl resulted from the weathering of evaporates and other minerals sediments in the aquifer. The aquifer sediments are composed of non-carbonate minerals such as pyrite (FeS), coquimbite ($AlFe_3(SO_4)_6(H2O)_{12} \cdot 6H_2O$), and Despujolsite ($Ca_3Mn^{4+}(SO_4)_2(OH)_6 \cdot 3H_2O$) (Abd El Raheem, 2019). Such sulfur-bearing minerals explain the prevailing of SO_4 anions in water. Over-pumping of groundwater accelerates the weathering of these minerals. Ismaiel et al., 2012 pointed out the presence of gypsum, anhydrite and halite in the Quaternary sediments at Qena governorate. He also found about 0.61–1582 mg/L 4.59–360.63 mg/L of Cl and SO_4, respectively, as dissolved salts in these sediments.

Considerable variances of Na (CV = 74.7%) are probably related to the cation exchange in the aquifer. CAI1 and CAI2 values were negative in 2017 period (Table 1) indicating forward ion exchange. While in 1997 the CAI1 and CAI2 values were mostly positive indicating the reverse ion exchange. CAI1 and CAI2

Table 1 Descriptive analysis of groundwater data (all ions in mg/L except Pb & Cd in μg/L)

Parameter	WHO 2017	Min		Max		Mean ± SD		10%	
		1997	2017	1997	2017	1997	2017	1997	2017
Depth	–	18.0	10.0	135.0	305.0	56.9 ± 26.2	49.4 ± 59.7	28.5	18.8
pH	6.5–8.5	7.2	7.1	8.4	8.1	8.0 ± 0.3	7.5 ± 0.3	7.6	7.2
TDS	1000	204.8	495.0	6412.8	4851.0	1280.6 ± 997.2	1828.6 ± 1124.7	595.2	561.0
EC	1500	320.0	904.3	10,020.0	8840.0	2000.9 ± 1558.1	3397.7 ± 2173.6	930.0	1044.0
T °C	–	14.2	26.3	32.8	32.1	25.8 ± 5.5	29.4 ± 1.6	16.9	26.9
Ca	75	16.0	15.0	359.0	214.2	88.0 ± 66.6	82.3 ± 57.2	33.6	23.4
Mg	100	11.0	10.0	236.0	120.3	52.9 ± 37.0	44.0 ± 25.4	22.2	19.4
Na	250	17.0	132.2	377.0	2718.6	131.5 ± 84.6	685.7 ± 512.0	53.0	183.3
K	12	1.2	2.9	10.0	43.5	4.5 ± 1.9	9.7 ± 8.0	2.5	3.5
HCO3	–	0.0	135.5	427.0	613.0	208.1 ± 89.7	318.5 ± 106.8	97.0	196.4
SO4	250	28.0	50.0	548.0	2750.0	148.1 ± 93.2	639.3 ± 587.0	60.0	97.0
Cl	250	0.0	62.0	1590.0	2215.6	298.7 ± 261.8	624.6 ± 475.1	70.8	127.6
NO3	50	–	0.0	–	417.6	–	102.3 ± 111.2	–	9.7
Pb	10	–	124.0	–	354.0	–	200.3 ± 60.3	–	138.4
Cd	3	–	0.0	–	17.0	–	6.5 ± 4.7	–	1.0
RI	–	0	0.2	40.2	14.2	3.3 ± 5.2	3.9 ± 3.6	0.4	0.7
CAI1	–	− 1.8	− 3.8	0.9	− 0.1	0.1 ± 0.5	− 0.9 ± 0.7	− 0.4	− 1.7
CAI2	–	− 2.2	− 1	5.9	− 0.1	0.4 ± 1	− 0.6 ± 0.2	− 0.2	− 0.8

Parameter	L.q		Median		U.q		90%		CV%	
	1997	2017	1997	2017	1997	2017	1997	2017	1997	2017
Depth	42.3	20.0	50.0	30.0	63.8	60.0	96.0	76.0	46.0	121
pH	7.8	7.3	8.0	7.6	8.2	7.7	8.3	8.0	3.5	3.5
TDS	659.2	946.0	924.8	1507.0	1468.8	2607.0	2534.4	3225.2	77.9	61.5
EC	1030.0	1674.6	1445.0	2680.8	2295.0	4746.7	3960.0	7263.7	77.9	64
T °C	20.7	28.0	28.1	29.5	29.1	30.6	32.0	31.6	21.4	5.5
Ca	49.0	46.8	68.2	65.4	93.5	84.3	168.4	194.9	75.6	69.5
Mg	29.4	26.9	44.5	40.0	60.4	52.9	101.6	76.9	70.1	57.6
Na	73.5	350.0	101.5	537.7	161.5	875.0	265.5	1464.5	64.3	74.7
K	3.2	5.0	4.2	6.4	6.0	11.2	7.0	20.7	41.2	82.4
HCO3	136.7	232.0	219.3	308.1	256.2	381.3	325.6	473.0	43.1	33.5
SO4	85.3	200.0	118.0	500.0	200.0	820.0	266.0	1382.0	63.0	91.8
Cl	144.0	281.0	220.2	514.0	416.5	797.6	646.1	1505.0	87.6	76.1
NO3	–	30.3	–	63.6	–	134.4	–	301.2	–	108.7
Pb	–	163.0	–	184.0	–	222.0	–	320.6	–	30.1
Cd	–	2.5	–	5.0	–	10.0	–	13.6	–	71.2
RI	0.9	1.8	2	2.9	3.6	4.7	6.2	8.6	157.6	92.3
CAI1	0	− 1	0.2	− 0.8	0.4	− 0.5	0.6	− 0.3	548.4	− 78.3
CAI2	0.7	− 0.5	0.2	− 0.6	0.7	− 0.5	1.3	− 0.3	241.2	− 34.8

Min. = Minimum, Max. = Maximum, SD = Standard Deviation, L.q = lower quartile Q1, U.q = upper quartile Q3, 10%, 90% = percentiles, C.V% = Coefficient of variation & RI = Revelle salinization index, the number of samples (n) was 66 for 1997 and 43 for 2017
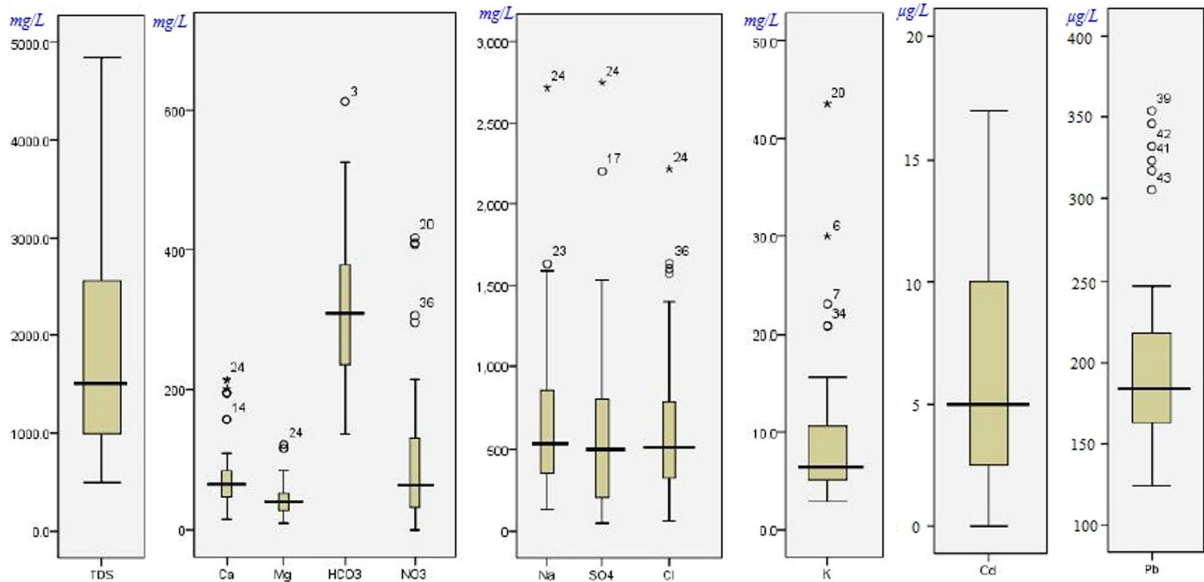
Fig. 3 A box-Whisker graph shows the variation of hydrochemical parameters (2017) in the aquifer system

values close to zero in 1997 refer to the restricted ion exchange in this period. Uniform pattern of HCO_3^- was indicated by narrow range of variation (CV = 35.5%) reflected on the condensed box-whisker graph (Fig. 3). This marked homogeneity implies the predominance of natural processes controlling HCO_3^- concentration and the limitations of anthropogenic effects. More than 50% of NO_3 values are above the WHO recommended limit (50 mg/L). The large nitrate dispersion is statistically proven, where the interquartile range (IQR) representing 50% of the central samples is significantly high (IQR = 104.1 mg/L). Such marked heterogeneity is reflected on the apparently scattered plots in the box-whisker graph (Fig. 3). Similarly, Cd and K exhibited considerable coefficient of variation (CV = 71.2 and 82.4%, respectively). These components most probably are supplied into the aquifer from different sources, such as agrochemicals and infiltrated domestic wastewater. Cd and Pb content is an obstacle to potable water. Pb content is almost constant along the whole aquifer area as indicated by its weak variance (CV% = 30.1%), suggesting its natural origin. Groundwater samples exhibited anomalous values (Fig. 3) are located next to the disposal sites (Sample No. 41&42) and in rural residential communities (villages) affected by anthropogenic activities. Some of these samples (No.3, 6, 7,

14, 17, 20, and 23) were collected from shallow wells (15–30 m).
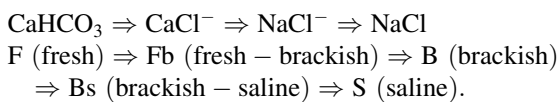
Hydrochemcial facies

RockWare Aq.QA software is widely used to study the geochemical evolution of groundwater, in terms of hydrochemical facies and water origin. In 1997, the groundwater types were Na–Cl (44%), Ca–Cl (13.7%), Mg–Cl (13.6%), Na-HCO3 (13.6%), Ca-CHO3 (3.1%), Mg-CHO3 (3.0%), Na-SO4 (4.5%), and Ca-SO4 (4.5%) water types. In 2017 the majority of the water belongs to Na-Cl facies (77%), whereas 14% is of Na-HCO3 and 9% of Na-SO4 types. Different water types (Ca–Cl, Mg–Cl, Na–Cl, and Na-HCO3) refer to different ion exchange processes formed through varied contact between freshwater and saltwater (Said et al., 2020). Generally, Na-Cl water type indicates a strong saltwater intrusion (Walraevens & Van Camp, 2004 and Calderon et al., 2014), while Ca–Cl and Mg–Cl facies results from ion-exchange due to mixing of freshwater with saltwater (Alfarrah & Walraevens, 2018; Appelo & Postma, 2005). Since the dominant anion (Cl) remains the same, the water type changes from Na–Cl to Mg–Cl and Ca–Cl, as a result of ion exchange (Said & Salman, 2021). Thereby the dominance of Na–Cl, Ca–Cl and Mg–Cl species in group A (Fig. 4) reflects aquifer salinization
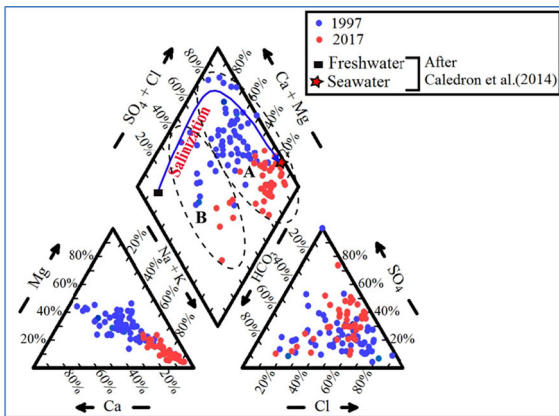
Fig. 4 Piper diagram of the studied groundwater (After Calderon et al., 2014)

via upconing of deep saline water, that connate saltwater associated with earlier transgression periods, which is usually trapped within clay and silt layers. Dissolution of chloride-rich sediments (surface saline wadis deposits and Pliocene marine sediments underneath) is another possible reason for salinization and elevated chloride content in group A (Rizk, 2010 and Said et al., 2020). Accordingly, the water types have evolved from low mineralized Ca-HCO₃, Mg-HCO₃, Na-HCO₃, Ca–Cl, Mg–Cl in 1997 to highly mineralized Na–Cl water types in 2017. Hence the proportion of Na–Cl facies expanded from 44% in 1997 to 77% in 2017, the matter explains the salinization process over time. Such salinization process can be schematized as follows (Jeen et al., 2001 and Alfarrah & Walraevens, 2018).

$CaHCO_3 \Rightarrow CaCl^- \Rightarrow NaCl^- \Rightarrow NaCl$
F (fresh) $\Rightarrow$ Fb (fresh − brackish) $\Rightarrow$ B (brackish) $\Rightarrow$ Bs (brackish − saline) $\Rightarrow$ S (saline).
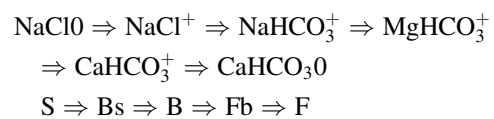
The scheme is also picturing how the reverse ion exchange (1997) evolved into a forward one (2017), which led to the predominance of sodium water.

Pleistocene aquifer is originally freshwater formed by rainwater and river Nile (Appelo & Postma, 2005; Said, 1962, 1990). It has undergone an upconing process from underlain saline aquifers along fault planes as a result of over-pumping. The Pleistocene aquifer is hydraulically connected with the deeper aquifers through a set of faults crossing the study area (RIGW, 1997 and Ismail et al., 2005, Gaber et al., 2020). Generally, the groundwater withdrawal rate

exceeds the recharge rate. The proportion of groundwater withdrawals to total renewable in Egypt is estimated as 350% (Giordano, 2009). All of this creates hydraulic gradients that encourage the upflowing of deep saline water toward Pleistocene freshwater, causing salinization. The saline water rises by 40 units for every unit of freshwater withdrawn as a result of over-extraction (Velmurugan et al., 2020). Recharging of Pleistocene aquifer from the aquifers underneath has been reported in previous studies in different Egyptian regions, among these Korany, 1984, Awad et al., 1995, Abdel Latif & El Kashouty, 2010, Sharaky et al., 2017 & Said & Salman, 2021.

Na^+/Cl^- vs Ca^{+2}/HCO_3^- ratio is taken as a reference parameter for the intrusion/freshening process (Appelo & Postma, 2005). Deficiency of Na^+/Cl^- (0.46 meq/l) and enrichment of Ca^{+2}/HCO_3^- ratio (averaging 1.57) revealed ion-exchange reaction during salinization process. Because in the case of intrusion process Na is adsorbed on the exchanger releasing calcium, so the ratio of Na^+/Cl^- decreases while the ratio of Ca^{+2}/HCO_3^- increases. That is why samples within group A (of water types Ca–Cl and Mg–Cl) are shifted to the right in a plot for $Ca^{+2} + Mg^{+2}$ to $Na^+ + K^+$ (Fig. 4), due to excess of Ca^{+2} and Mg^{+2}.

The opposite is true in case of the freshening process (group B), where Ca and/or Mg are adsorbed while Na releases. Group B predominate over Na-HCO₃, Ca-HCO₃, and Mg-HCO₃ facies indicating freshwater in nature and meteoric recharge system. These wells are located close to the flood plain boundaries, and most of them under shallow conditions (15- 30 m) recharged from irrigation canals. Na-HCO₃ water samples were formed by an ion-exchange reaction during the flushing of saltwater. As a result Na^+/Cl^- ratio increases (averaging 1.26) while Ca^{+2}/HCO_3^- ratio decreases (averaging 0.23), where Ca^{+2} is uptaken by exchanger releasing Na^+ causing a surplus of Na^+ and depletion of Ca^{+2}. The freshening process can be schematized as follows (Walraevens & Van Camp, 2004)

$NaCl0 \Rightarrow NaCl^+ \Rightarrow NaHCO_3^+ \Rightarrow MgHCO_3^+$
$\Rightarrow CaHCO_3^+ \Rightarrow CaHCO_30$
$S \Rightarrow Bs \Rightarrow B \Rightarrow Fb \Rightarrow F$

Moreover, enrichment of Na^+/Cl^- (averaging 1.26) vs the deficiency of $Ca^{2+} + Mg^{2+}/SO_4^{-2} + HCO_3^-$

(0.16 meq/l), confirms the ion exchange process predominating in Na-CHO₃ water samples within group B (Fig. 4). It's well known that the molar ratio ($Ca^{2+} + Mg^{2+}/SO_4^{-2} + HCO_3^{-}$) derived from dissolution of carbonate and sulfate minerals equals 1:1, similarly Na^{+}/Cl^{-} molar ratio for halite (Ledesma-Ruiz et al., 2015). The deviation from these standard ratios here is due to the ion exchange process. Where Na^{+} adsorbed on the clay surface is successively replaced by Ca^{2+-} ions due to increased affinity for clay. Such process can be schematized as follows:

$$2Na^{+}Clay + Ca^{+2}, Mg^{2+}$$
$$\Rightarrow Ca^{+2}, Mg^{2+}Clay + 2Na^{+}$$
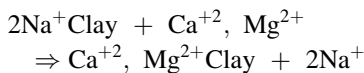
Aquifer salinization over time

Geochemical evolution of groundwater facies over time has increased the aquifer salinity. TDS distributions were compared between years 1997 and 2017 (Fig. 5). The increase in salinity over time from 1997 to 2017 was statistically documented at P value < 0.05 using independent samples t test. Very high significance < 0.05 indicates there is statistical difference between the two means of salinity over twenty years (1280 mg/L at 0.008 in 1997 and 1828 mg/L at 0.01 in 2017). Revelle salinization index (Revelle, 1941) with average values of 3.3 and 3.9, for 1997 and 2017, respectively, confirmed an increase in groundwater salinity over time. Figure 5 showed that about
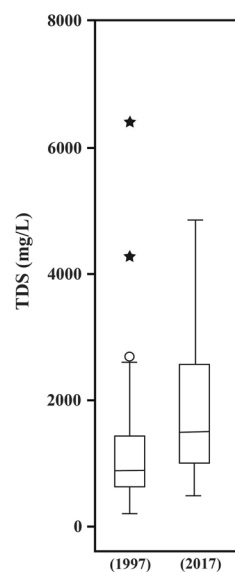
25% of the wells in 2017 had expanded to higher TDS levels than the highest TDS in 1997 (especially when the two upper outliers are excluded). This quartile is located between U.q = 2607 and maximum (4852 mg/L). The matter means that a quarter of the aquifer area has been subjected to salinization within 20 years. Drinkable water has decreased by 25% in twenty years. In 1997, 50% of the wells had lower salinity and were drinkable (WHO 2017), compared to only 25% in 2017 (Table 1 and Fig. 5). Such deterioration of the groundwater quality over time shows the impact of anthropogenic influences on the evolution of groundwater salinity. The expansion of agricultural activities during 1984–2018 (Kamel, 2020) resulted in increased groundwater withdrawal, enhancing saline-water intrusion from the aquifers underneath causing salinization. Saudi Arabia has a similar negative story in using groundwater to planting deserts. In Egypt, most of the wells used in farms on the Cairo-Alexandria desert road have become salinized. The use of groundwater in desert agriculture is the least economically choice, given that it is non-renewable, deep, and costly. The use of groundwater for industrial purposes is the most logical choice; less water wastage and more share in GDP. Agriculture consumes 85% of the total water resources while the industrial sector does not exceed 10%, but shares in GDP of the country 10 times more than the agricultural sector (Mohamed, 2021).

Principle component analysis (PCA)

The component matrix to define basic hydrochemical processes is provided in Table 2. Values in bold refer to the highest loading variables in each factor. Setting 0.5 as a base value is to ensure neutrality in dealing with the results of the statistical model. Four principles components (PCs) represent about 78% of the total variance. PC1 explaining over 46% of the variance had high loading with Na, Ca, Mg, Cl, SO₄, NO₃, Cd, and TDS. The general behavior of exchangeable ions markedly follows the same TDS trend suggesting the mineralization process as the main salinity source. Gibbs (1970) and Gaillardet et al. (1999) (Fig. 6) indicate dissolution of salts-bearing sediments; evaporites are the major factor responsible for the hydrochemical characteristic of the groundwater in 2017 while in 1997 silicate weathering is more effective as the long time contact with silicate. The flow of

Fig. 5 Increasing salinity of groundwater in Luxor area (1997–2017)

Table 2 Component matrix[a] of groundwater data

Variable	Principal component loadings			
	PC1	PC2	PC3	PC4
Depth	− 0.205	− 0.088	0.416	**0.726**
pH	− 0.220	**.705**	0.268	0.191
TDS	**0.922**	0.294	0.131	− 0.023
Ca	**0.917**	− 0.181	− 0.063	0.059
Mg	**0.833**	− 0.064	− 0.032	− 0.076
Na	**0.913**	0.012	0.230	− 0.114
K	0.424	0.154	**− 0.691**	0.193
HCO₃	− 0.189	**0.576**	0.006	**− 0.508**
SO₄	**0.903**	− 0.106	0.200	− 0.042
Cl	**0.920**	0.007	0.170	− 0.042
NO₃	**0.546**	0.008	**− 0.627**	0.254
Pb	0.249	**− 0.664**	0.255	− 0.171
Cd	**0.735**	**0.500**	0.182	0.173
Eigenvalues	6.086	1.686	1.358	1.008
Variance%	46.813	12.971	10.449	7.755
Cumulative%	46.813	59.784	70.233	77.988

Extraction Method: Principal Component Analysis

Kaiser–Meyer–Olkin Normalization (KMO = 0.659)

a. 4 components extracted

samples from rock dominance into evaporation dominance gives an indication on saltwater intrusion. Excessive pumping accelerated saltwater intrusion resulting in groundwater deterioration. On the other hand, the weak negative depth loading of the mineralizing factor (PC1) indicates the partial contribution of surface leaching to the salinization process; in return, it supports the possibility of masked saltwater upconing from the deeper aquifers. Therefore, the salinization process is controlled by different mechanisms are an intrusion of saltwater from the underline aquifer, dissolution of evaporitic minerals from the bottom aquifer sediments, and migration of salts from the surface soil with surplus irrigation water, all activate ion exchange and increase Na concentration in the groundwater enhancing groundwater salinization. (Na/(Ca + Na)) > 0.5 on Gibbs diagram (Fig. 6a) showing an ion exchange, more obvious in 2017 which has changed the water type into Na-rich water causing aquifer salinization. The Na/(Ca + Na) ratio is < 1 for all samples (Fig. 6a) indicating silicate weathering (Sunkari et al., 2021). Silicate weathering and reverse ion exchange was prevailing in 1997 but in 2017 Na⁺ concentration increased about 5 times (685.7) more than in 1997 (131.5 mg/L), due to the
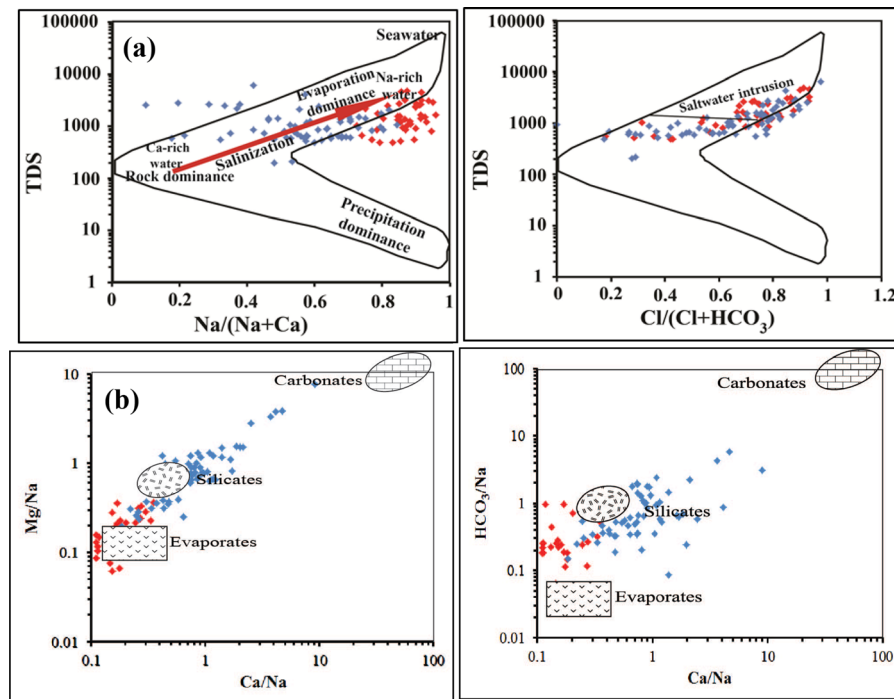
Fig. 6 Groundwater geochemistry based on **a** Gibbs diagram and **b** End-member plot

dissolution of evaporates and saltwater intrusion under over-pumping. The dissolution of evaporitic minerals is indicated from Fig. 6 and saturation index (SI) results. SI values of halite ranged from − 6.5 to − 4.0 averaging − 5.2 whereas gypsum SI ranged from − 2.5 to − 0.5 averaging − 1.4. Halite under-saturation explains the role of evaporate weathering in groundwater chemistry. This dissolution enriches the groundwater with Na^+ and $Cl^−$ ions, which increases the aquifer salinity.

From the above, it is clear that the dissolution of marine sediments and upconing of deep saline water are the main aquifer salinization mechanisms. The implication of over-irrigation as a common factor between those two mechanisms can be extrapolated as follows: Cd and Nitrate are usually considered as marker elements of agricultural activities. Coupling of cadmium and nitrates with TDS (PC1) supports the responsibility of the intensive agricultural activity for mineralization/salinization process. Excessive pumping accelerated saltwater intrusion along the fault planes resulting in groundwater degradation. On the other hand, pumping too much accelerates the weathering of sediments in contact, enriching the aquifer system with salts. Leaching of salts from overlain saline soil with irrigation return and dissolution of Pliocene marine clay underneath lead to the aquifer salinization (Rizk, 2010 and Said et al., 2020).

PC2 accounts for 12.9% of the total variance, it comprised Cd and $HCO_3^−$ in negative correlation with Pb, in such case, leaching of Cd with the percolating water is suspected. Cd enrichment in the bioavailable fraction refers to anthropogenic sources. The considerable variance of Cd (CV = 71.2%) is another evidence of anthropic origin. That's why Pb existed in negative correlation with Cd and $HCO_3^−$ on PC2 forming an independent trend (different origin). Because Pb has a lower coefficient of variation (low CV = 33%) and is mainly precipitated in the carbonate phase, which is likely natural origin. Lead substitution for Cd in carbonate phase is another possible explanation.

PC3 (10.4%) links K^+ and $NO_3^−$, refers to the effect of fertilization or domestic wastewater infiltration on the behavior of $NO_3^−$ and K^+. Presence of Nitrate and Cd in more than one factor confirms their mixed origin. Nitrate and Potassium could be supplied into the aquifer through infiltration of agrochemicals as well as domestic wastewater containing nitrogen compounds and K-bearing household materials. PC4 contributed only 7.5% of the total variances and is mainly involved by $HCO_3^−$ negatively correlated with depth, suggesting meteoric recharge. Bicarbonate could be brought into the aquifer through infiltrating of CO_2-bearing meteoric water. Na-HCO_3 water type in the previous section refers to the natural recharge from irrigation surplus and domestic wastewater. It can be said that PC1 is corresponding to water group A (salinization group), while PC2–PC4 represents recharge group B.

Speciation and bioavailability

When saltwater mixes with freshwater a large number of physical and chemical phases take place which affects the distribution of PTEs over particulate and dissolved phase (Salomons & Förstner, 2012). This in turn affects the level of toxicity. Geochemical speciation model using visual MINTEQ 3.1 has been applied here, to predict the different species of Cd and Pb in groundwater, to identify their bioavailability. The results indicated that the majority of Cd exists in mobile species bioavailable for plants alarming environmental situation. While lead is precipitated mainly in the carbonate phase, indicating less potential ecological risk. Potential bioavailability of Cd (based on dissolved ions %) ranged from 64 to 93.3% averaging 83.6%. Cadmium as free (Cd^{2+}) was bioavailable at 47.1% of its total concentration and 36.5% as complex ion ($CdCl^+$ species). Chlorides have a high affinity for forming soluble complexes with Cd (Kabata-Pendias, 2010) facilitate Cd-plant uptake. Table 3 showed $CdCl^+$ species in positive correlation with TDS and chloride ($r = 0.33$ and 0.3, respectively at P-value < 0.05) reflects the role of salinity and chlorinity in Cd mobility (Salomons & Förstner, 2012). Thus even in alkaline soil with

Table 3 Pearson correlation for $CdCl^+$, TDS, and Cl

	$CdCl^+$	TDS	Cl
$CdCl^+$	1	0.332*	0.302*
TDS	0.332*	1	0.904**
Cl	0.302*	0.904**	1

*Correlation is significant at the 0.05 level (2-tailed)

**Correlation is significant at the 0.01 level (2-tailed)

opposing charges, elevated salinity is expected to keep $CdCl^+$ in bioavailable form, by providing competing major ions preventing its adsorbing on the soil adsorption sites. Although Cd concentration is close to FAO's limits (0.01 mg/L), its anthropogenic origin alarms possible toxic level over time. The potential bioavailability of Pb was estimated by 23.9% on average; 7% existed as free ions (Pb^{+2}) and 17.9% as complexes ions with anions such as OH^-, HCO_3^-, and Cl^-. While 70.8% of lead is precipitated as $PbCO_3$ species. Precipitation of lead predominantly in $PbCO_3$ species reduces Pb-contamination risk to biota, because of restricted mobility. However, under acidic conditions, Pb will get bioavailable.

Conclusion

Groundwater salinization is a complex insidious process being related to a variety of physical mechanisms. The matter has required integration between all possible environmental parameters using multivariate statistics and hydrochemical models to reveal the causes of salinization in Luxor area. The hydrochemical data indicated that Pleistocene aquifer is of meteoric origin, and it was mixed with saline water under intensive irrigation, which led to a change in the type of salts and an increase in salinity. 25% of the aquifer was devoured by salinization during 20 years. Groundwater quality was holding a bit by silicate weathering in 1997 and then changed through evaporites dissolution (saltwater intrusion) in 2017. Excessive pumping accelerated saltwater intrusion resulting in groundwater deterioration. The Statistical conjugation of cadmium and nitrate with salinity indicated the responsibility of agricultural activities for aquifer salinization. The weak negative loading of depth in the mineralization process indicates surface activities are partially participating in the aquifer salinization and refers to a masked upconing process. The salinization process led to aquifer acidification and cadmium mobilization through the forming of a soluble $CdCl^+$ complex. The expansion in desert land reclamation and associated over-pumping of groundwater must be restricted. The use of groundwater for industrial purposes is the most logical option, being less water consumption and more share in GDP compared to the agricultural sector. Construction of new communities instead of agriculture, and/or use of modern agricultural irrigation techniques should be applied; hence, the aquifer is less exposed to degradation (salinization, acidification, and pollution). The lack of an environmental database is one of the main causes of the problem, so periodic environmental monitoring is recommended to help early detection of an environmental problem before it worsens.

Declarations

References

Abd El Raheem, S. M. (2019). *Geochemical and mineralogical characteristics of Nile sediments and their impacts on water quality in the Quaternary aquifer, Sohag area*. Sohag University, Egypt.

Abd Ellah, R. G. (2020). Water resources in Egypt and their challenges, Lake Nasser case study. *The Egyptian Journal of Aquatic Research, 46*(1), 1–12.

Abdel Latif, A., & El Kashouty, M. (2010). Groundwater investigation in Awlad Salameh, Southern Sohag. *Upper Egypt. Earth Sciences Research Journal, 14*(1), 63–75.

Abd-Elhamid, H., Javadi, A., Abdelaty, I., & Sherif, M. (2016). Simulation of seawater intrusion in the Nile Delta aquifer under the conditions of climate change. *Hydrology Research, 47*(6), 1198–1210.

Abdel-Shafy, H. I., & Kamel, A. H. (2016). Groundwater in Egypt issue: Resources, location, amount, contamination, protection, renewal, future overview. *Egyptian Journal of Chemistry, 59*(3), 321–362.

Alfarrah, N., & Walraevens, K. (2018). Groundwater overexploitation and seawater intrusion in coastal areas of arid and semi-arid regions. *Water, 10*(2), 143.

Appelo, C. A. J., & Postma, D. (2005). *Geochemistry, groundwater and pollution* (2nd ed.). Balkema.

Awad, M. A., Nada, A. A., Hamza, M. S., & Froehlich, K. (1995). Chemical and isotopic investigation of groundwater in Tahta region, Sohag-Egypt. *Environmental Geochemistry and Health, 17*(3), 147–153.

Bocanegra, E., Da Silva, G. C., Custodio, E., Manzano, M., & Montenegro, S. (2010). State of knowledge of coastal aquifer management in South America. *Hydrogeology Journal, 18*(1), 261–267.

Calderon, H., Weeda, R., & Uhlenbrook, S. (2014). Hydrological and geomorphological controls on the water balance components of a mangrove forest during the dry season in the Pacific Coast of Nicaragua. *Wetlands, 34*(4), 685–697.

CAPMAS. (2020). *Water Balance For Egypt (15/16 - 18/2019). Egypt in Figures.* https://www.capmas.gov.eg/Pages/Publications.aspx?page_id=5104&Year=23608

EGSM (Egyptian Geological Survey and Mining Authorities). (1981). The geological map of Egypt. Scale 1: 2000000. *Ministry of industry and mineral resources, 1.*

El Alfy, M., Abdalla, F., Moubark, K., & Alharbi, T. (2019). Hydrochemical equilibrium and statistical approaches as effective tools for identifying groundwater evolution and pollution sources in arid areas. *Geosciences Journal, 23*(2), 299–314.

El-Gohary, E. F. (2011). Integration of Wastewater in the Water Resources of Egypt: Opportunities and Constrains. *on Water, Energy and Environment 2011*, 179.

Elwaseif, M., Ismail, A., Abdalla, M., Abdel-Rahman, M., & Hafez, M. A. (2012). Geophysical and hydrological investigations at the west bank of Nile River (Luxor, Egypt). *Environmental Earth Sciences, 67*(3), 911–921.

Essink, G. H. P. O. (2001). Saltwater intrusion in 3D large-scale aquifers: A Dutch case. *Physics and Chemistry of the Earth, Part b: Hydrology, Oceans and Atmosphere, 26*(4), 337–344.

FAO. (1994). *Water Quality for Agriculture.* http://www.fao.org/3/t0234e/T0234E00.htm#TOC

FAO. (2011). *The state of the world's land and water resources for food and agriculture—managing systems at risk.* Food and Agriculture Organization of the United Nations and Earthscan.

FAOSTAT. (2016). FAO Food and Agriculture Database. *Statistics Divi sion, Food and Agriculture Organization of the United Nations.* http://www.fao.org/faostat/en/#home

Foster, S., Pulido-Bosch, A., Vallejos, Á., Molina, L., Llop, A., & MacDonald, A. M. (2018). Impact of irrigated agriculture on groundwater-recharge salinity: A major sustainability concern in semi-arid regions. *Hydrogeology Journal, 26*(8), 2781–2791.

Gaber, A., Mohamed, A. K., ElGalladi, A., Abdelkareem, M., Beshr, A. M., & Koch, M. (2020). Mapping the groundwater potentiality of West Qena Area, Egypt, using integrated remote sensing and hydro-geophysical techniques. *Remote Sensing, 12*(10), 1559.

Gaillardet, J., Dupré, B., Louvat, P., & Allegre, C. J. (1999). Global silicate weathering and CO2 consumption rates deduced from the chemistry of large rivers. *Chemical Geology, 159*(1–4), 3–30.

Gibbs, R. J. (1970). Mechanisms controlling world water chemistry. *Science, 170*(3962), 1088–1090.

Giordano, M. (2009). Global groundwater? Issues and solutions. *Annual Review of Environment and Resources, 34*, 153–178.

Greene, R., Timms, W., Rengasamy, P., Arshad, M., & Cresswell, R. (2016). Soil and aquifer salinization: toward an integrated approach for salinity management of groundwater. In A. J. Jakeman, O. Barreteau, R. J. Hunt, J.-D. Rinaudo, & A. Ross (Eds.), *Integrated groundwater management* (pp. 377–412). Cham: Springer.

Gustafsson, J. P. (2011). Visual MINTEQ Version 3.1: A Windows version of MINTEQA2.

EL HALIMI, N., CHAOUNI ALIA, A., Beeuwsaert, E., & Walraevens, K. (2001). Hydrogeological and geophysical investigation for characterizing the groundwater reservoir in Saidia Plain (northeastern Morocco). In *Development of water resource management tools for problems of seawater intrusion and contamination of fresh-water resources in*

coastal aquifers/Walraevens, K.(ed.).-Gent: Ghent University, 2000.-ISBN 90-76878-01-3 (pp. 67–75).

Ismaiel, H. A. H., Askalany, M. M., & Ibrahim, A. M. (2012). Geotechnical classification of quaternary sediments exposed along Qena-Safaga, Qift-Quseir and Qena-Nag Hammadi roads at Qena region, Egypt. In *Conference program and abstracts, geology of the Nile basin countries conference. Egypt, Alexandria.*

Ismail, A., Anderson, N. L., & Rogers, J. D. (2005). Hydrogeophysical investigation at Luxor, southern Egypt. *Journal of Environmental & Engineering Geophysics, 10*(1), 35–49.

Jeen, S.-W., Kim, J.-M., Ko, K.-S., Yum, B., & Chang, H.-W. (2001). Hydrogeochemical characteristics of groundwater in a mid-western coastal aquifer system. *Korea. Geosciences Journal, 5*(4), 339–348.

Jolliffe, I. T., & Cadima, J. (2016). Principal component analysis: A review and recent developments. *Philosophical Transactions of the Royal Society a: Mathematical, Physical and Engineering Sciences, 374*(2065), 20150202.

Kabata-Pendias, A. (2010). *Trace elements in soils and plants.* CRC Press.

Kaiser, H. F. (1960). The application of electronic computers to factor analysis. *Educational and Psychological Measurement, 20*(1), 141–151.

Kamel, M. (2020). Monitoring of land use and land cover change detection using multi-temporal remote sensing and time series analysis of Qena-Luxor Governorates (QLGs), Egypt. *Journal of the Indian Society of Remote Sensing, 48*(12), 1767–1785.

Karunanidhi, D., Aravinthasamy, P., Deepali, M., Subramani, T., & Sunkari, E. D. (2020). Appraisal of subsurface hydrogeochemical processes in a geologically heterogeneous semi-arid region of south India based on mass transfer and fuzzy comprehensive modeling. *Environmental Geochemistry and Health, 43*, 1–20.

Kaur, L., Rishi, M. S., Sharma, S., Sharma, B., Lata, R., & Singh, G. (2019). Hydrogeochemical characterization of groundwater in alluvial plains of River Yamuna in Northern India: An insight of controlling processes. *Journal of King Saud University-Science, 31*(4), 1245–1253.

Korany, E. (1984). Statstical approach in the assessment of the geohydrologic profiles. In *9th International Congress. Statistics, Computer. Sciences. Social and Demerges Research, Cairo.* Ain Shams University Press.

Krishan, G. (2019). Groundwater salinity. *CurRent World Environment, 14*(2), 186.

Ledesma-Ruiz, R., Pastén-Zapata, E., Parra, R., Harter, T., & Mahlknecht, J. (2015). Investigation of the geochemical evolution of groundwater under agricultural land: A case study in northeastern Mexico. *Journal of Hydrology, 521*, 410–423.

Margat, J., & der Gun, J. (2013). *Groundwater around the world: a geographic synopsis.* Boca Raton: Crc Press.

Mazzoni, A., Heggy, E., & Scabbia, G. (2018). Forecasting water budget deficits and groundwater depletion in the main fossil aquifer systems in North Africa and the Arabian Peninsula. *Global Environmental Change, 53*, 157–173.

Mohamed, N. N. (2021). Optimum Economic Uses of Precious Costly Ground Water in Marginal and Desert Lands; Case Study in Egypt. In A. Negm & A. Elkhouly (Eds.),

Groundwater in Egypt's Deserts (pp. 373–393). Cham: Springer.

Morris, B. L., Lawrence, A. R. L., Chilton, P. J. C., Adams, B., Calow, R. C., & Klinck, B. A. (2003). Groundwater and its susceptibility to degradation: A global assessment of the problem and options for management. http://nora.nerc.ac.uk/id/eprint/19395/1/Groundwater_INC_cover.pdf.

Mostafa, A. N., Wheida, A., El Nazer, M., Adel, M., El Leithy, L., Siour, G., et al. (2019). Past (1950–2017) and future (-2100) temperature and precipitation trends in Egypt. *Weather and Climate Extremes, 26*, 100225.

Omer, A. A. (1996). *Geological, mineralogical and geochemical studies on the Neogene and Quaternary Nile basin deposits, Qena-Assiut stretch, Egypt*. Ph. D. thesis, Geology Dept. Faculty of Science, Sohag, South Valley University.

Omran, A. A., Riad, S., Philobbos, E. R., & Othman, A. B. (2001). Subsurface structures and sedimentary basins in the Nile Valley area as interpreted from gravity data. *Egyptian Journal of Geology, 45*(1), 681–712.

Piper, A. M. (1944). A graphic procedure in the geochemical interpretation of water-analyses. *Eos, Transactions American Geophysical Union, 25*(6), 914–928.

Pulido-Bosch, A., Rigol-Sanchez, J. P., Vallejos, A., Andreu, J. M., Ceron, J. C., Molina-Sanchez, L., & Sola, F. (2018). Impacts of agricultural irrigation on groundwater salinity. *Environmental Earth Sciences, 77*(5), 1–14.

Revelle, R. (1941). Criteria for recognition of the sea water in ground-waters. *Eos, Transactions American Geophysical Union, 22*(3), 593–597.

RIGW (Research Institute of Groundwater). (1997). Hydrogeological map of Luxor area (Scale 1:100 000). *Explanatory notes*, 23.

Rizk, S. (2010). *Assessment of groundwater quality in sohag governorate, Egypt. A study in the environmental geochemistry*. Sohag: South Valley University.

Said, I., Merz, C., Salman, A., Schneider, M., & Winkler, A. (2020). Identification of hydrochemical processes using multivariate statistics in a complex aquifer system of Sohag region Egypt. *Environmental Earth Sciences*. https://doi.org/10.1007/s12665-020-08913-8

Said, I., & Salman, S. A. (2021). Salinization of groundwater under desert reclamation stress at Qena region, Egypt. *Journal of African Earth Sciences, 181*, 104250.

Said, R. (1962). *The Geology of Egypt*. Amsterdam: Elsevier book company.

Said, R. (1990). *The Geology of Egypt*. Rotterdam/Brookfield: AA Balkema.

Said, R. (2012). *The geological evolution of the River Nile*. Berlin: Springer Science & Business Media.

Salomons, W., & Förstner, U. (2012). *Metals in the Hydrocycle*. Berlin: Springer Science & Business Media.

Scanlon, B. R., Jolly, I., Sophocleous, M., & Zhang, L. (2007). Global impacts of conversions from natural to agricultural ecosystems on water resources: Quantity versus quality. *Water resources research, 43*(3), 1–18.

Schoeller, H. (1965). *Qualitative evaluation of groundwater resources* (p. 5483). UNESCO.

Sharaky, A. M., El Hassanein, A. S., Atta, S. A., & Khallaf, K. M. A. (2017). Salinization and origin of the coastal shallow groundwater aquifer, northwestern Nile Delta, Egypt. In A. M. Negm (Ed.), *Groundwater in the Nile Delta* (pp. 275–306). Cham: Springer.

Sherif, M. (1999). Nile delta aquifer in Egypt. In J. Bear, A.H.-D. Cheng, S. Sorek, D. Ouazar, & I. Herrera (Eds.), *Seawater Intrusion in Coastal Aquifers—Concepts, Methods and Practices* (pp. 559–590). Dordrecht: Springer.

Siebert, S., Burke, J., Faures, J.-M., Frenken, K., Hoogeveen, J., Döll, P., & Portmann, F. T. (2010). Groundwater use for irrigation–a global inventory. *Hydrology and Earth System Sciences, 14*(10), 1863–1880.

Sunkari, E. D., Abu, M., & Zango, M. S. (2021). Geochemical evolution and tracing of groundwater salinization using different ionic ratios, multivariate statistical and geochemical modeling approaches in a typical semi-arid basin. *Journal of Contaminant Hydrology, 236*, 103742.

Tabachnick, B. G., & Fidell, L. S. (2007). *Using multivariate statistics*. Boston: Allyn & Bacon/Pearson Education.

VAndenBOHede, A., WAlrAeVens, K., & De Breuck, W. (2015). What does the interface on the fresh-saltwater distribution map of the Belgian coastal plain represent? *Geologica Belgica, 18*(1), 31–36.

Velmurugan, A., Swarnam, P., Subramani, T., Meena, B., & Kaledhonkar, M. J. (2020). Water Demand and Salinity. In *Desalination-Challenges and Opportunities*. IntechOpen.

Walraevens, K., & Van Camp, M. (2004). Advances in understanding natural groundwater quality controls in coastal aquifers. In *Proceedings of the 18th Salt Water Intrusion Meeting* (Vol. 31, pp. 449–463).

Weaver, J. M. C. (1992). Groundwater Sampling Manual. WRC Report No. TT 54/92. *Water Research Commission, Pretoria*.

Werner, A. D. (2010). A review of seawater intrusion and its management in Australia. *Hydrogeology Journal, 18*(1), 281–285.

WHO (World Health Oraganization). (2017). *Guidelines for drinking-water quality: first addendum to the fourth edition*.

Williams, W. D. (2001). Anthropogenic salinisation of inland waters. In J. M. Melack, R. Jellison, & D. B. Herbst (Eds.), *Saline lakes* (pp. 329–337). Springer.

Yidana, S. M., Ophori, D., Yakubo, B. B., & Samed, A. A. (2012). A factor model to explain the hydrochemistry and causes of fluoride enrichment in groundwater from the middle Voltaian sedimentary aquifers in the northern region, Ghana. *ARPN J Eng Appl Sci, 7*(1), 50–68.